

Analyst

Accepted Manuscript



This is an *Accepted Manuscript*, which has been through the Royal Society of Chemistry peer review process and has been accepted for publication.

Accepted Manuscripts are published online shortly after acceptance, before technical editing, formatting and proof reading. Using this free service, authors can make their results available to the community, in citable form, before we publish the edited article. We will replace this *Accepted Manuscript* with the edited and formatted *Advance Article* as soon as it is available.

You can find more information about *Accepted Manuscripts* in the [Information for Authors](#).

Please note that technical editing may introduce minor changes to the text and/or graphics, which may alter content. The journal's standard [Terms & Conditions](#) and the [Ethical guidelines](#) still apply. In no event shall the Royal Society of Chemistry be held responsible for any errors or omissions in this *Accepted Manuscript* or any consequences arising from the use of any information it contains.

1
2
3
4
5
6
7
8
9
10
11 **Ionization characteristics of amino acids in direct analysis in real time**
12
13 **mass spectrometry**
14
15
16

17 Kanako Sekimoto^{1*}, Motoshi Sakakura², Takatomo Kawamukai², Hiroshi Hike², Teruhisa
18 Shiota², Fumihiko Usui², Yasuhiko Bando² and Mitsuo Takayama¹
19

20
21
22 ¹ Graduate School of Nanobioscience, Yokohama City University, 22-2 Seto, Kanazawa-ku,
23
24
25 Yokohama, Kanagawa, 236-0027 Japan
26

27 ² AMR Inc., 13-18 Nakane-2, Meguro-ku, Tokyo, 152-0031 Japan
28
29
30
31
32
33
34
35
36
37
38
39
40
41

42 ***Author for Correspondence**
43

44 Present address: Graduate School of Nanobioscience, Yokohama City University, 22-2 Seto
45
46
47 Kanazawa-ku, Yokohama, Kanagawa, 236-0027 Japan
48

49 Tel: +81-45-787-2216
50

51 E-mail: sekimoto@yokohama-cu.ac.jp
52
53
54
55
56
57
58
59
60

Abstract

The positive and negative ionization characteristics of 20 different α -amino acids were investigated in Direct Analysis in Real Time (DART) mass spectrometry. Almost all of the amino acids M were ionized to generate the (de)protonated analytes $[M \pm H]^\pm$ via proton transfer reactions with the typical background ions $H_3O^+(H_2O)_n$ and $O_2^{\cdot\cdot}$ and resonant electron capture by M . The application of DART to amino acids also resulted in molecular ion formation, fragmentation, oxidations involving oxygen attachment and hydrogen loss, and formation of adducts $[M + R]^-$ with negative background ions R^- ($O_2^{\cdot\cdot}$, HCO_2^- , NO_2^- and $COO^-(COOH)$), depending on the physicochemical and/or structural properties of the individual amino acid. The relationship between each amino acid and the ionization reactions observed suggested that fragmentation can be attributed to pyrolysis during analyte desorption, as well as excess energy obtained via (de)protonation. Oxidation and $[M + R]^-$ adduct formation, in contrast, most likely originate from reactions with active oxygen such as hydroxyl radical HO^\cdot , indicating that the typical background neutral species involved in analyte ionization in DART contain HO^\cdot .

Introduction

The recent development of ambient desorption/ionization (ADI) mass spectrometry offers numerous advantages, including direct analysis of solids and liquids under ambient conditions with little or no sample preparation. For these reasons, ADI sources have become important tools in cleaning validation,¹ forensic analysis,² and drug discovery.³ Although several different types of ADI sources have been developed so far, a large amount of interest has been placed on direct analysis in real time (DART) using a helium plasma source, which is the origin of ADI sources.⁴ DART combines separate desorption and ionization processes into a single method. The desorption is carried out using hot helium gases, whereas the ionization goes through an atmospheric pressure chemical ionization (APCI)-like process with reactions involving excited helium.^{5,6} It has been reported that DART is a soft ionization technique forming abundant (de)protonated analytes $[M \pm H]^\pm$ via proton transfer from background ions such as $H_3O^+(H_2O)_n$ and O_2^- to the analytes M ,^{4,5} while analytes with certain specific features can be ionized to form additional analyte ions. For instance, DART ionization of nonpolar compounds such as alkanes leads to the production of analyte ions originating from hydride abstraction, oxygen attachment, or hydrogen loss, instead of $[M \pm H]^\pm$.^{6,7} The mechanism of formation of those analyte ions is not well understood, although the involvement of NO^+ , one of the background ions in DART gas flow, has been suggested.⁶ A lack of knowledge concerning the ionization characteristics in DART results in difficulty in the interpretation of DART mass spectra, and limits its analytical utility. In order to overcome these issues, it is necessary to investigate the ionization characteristics of DART in detail, i.e., to identify the background ionic and neutral species

1
2
3
4
5
6 formed in DART sources and to systematically understand the influence of these individual
7
8 background compounds on analyte ionization.
9

10
11 Herein, the positive and negative ionization characteristics of 20 different α -amino acids
12
13 were investigated by DART mass spectrometry. The amino acids used have a wide variety of
14
15 physicochemical and/or structural properties originating from their side chains, including the
16
17 nonpolarity associated with aliphatic or aromatic character, and the polarity due to the presence
18
19 of specific functional groups (hydroxyl, amino, carboxyl and thiol groups). All of the amino
20
21 acids except for arginine were positively and negatively ionized via various different reactions
22
23 including (de)protonation, molecular ion formation, fragmentation, oxidation, hydrogen loss,
24
25 and the formation of adducts with negative background ions. The relationship between the
26
27 physicochemical and/or structural properties of the individual amino acids and ionization
28
29 reactions observed contributes to the understanding of the formation of background ionic and
30
31 neutral species and the resulting effects on analyte ionization in DART.
32
33
34
35
36
37
38
39
40
41
42
43
44
45
46
47
48
49
50
51
52
53
54
55
56
57
58
59
60

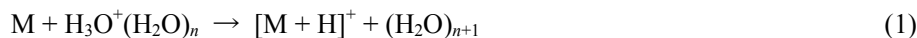
Experimental

All mass spectra were acquired with an LCQ ion-trap mass spectrometer (Thermo Fisher Scientific, San Jose, CA) equipped with a DART-SVP source (IonSense, Saugus, MA). The DART-SVP source was operated with a needle voltage of 5000 V and an exit grid electrode voltage of 350 V. Helium (He) at 350 °C was used for the DART gas at the factory-preset flow rate (2.5 Lmin⁻¹). The DART source exit was directed toward the orifice of the mass spectrometer, separated by a gap of \approx 10 mm. The analytes used were the 20 standard α -amino acids (Table 1), purchased from Sigma-Aldrich (Tokyo, Japan). Analyte desorption and ionization was accomplished by an insertion of a 1.5 mm i.d. glass tube containing the analyte in the He gas flow between the DART source exit and the mass spectrometer orifice. The resulting gas-phase analyte ions were introduced into the orifice. The orifice was heated at 275 °C and applied a voltage of 20 V. The ions were focused onto the skimmer and the tube lens and were transported into the ion-trap analyzer through ion guides consisting of a quadrupole, gate lens, octapole and entrance lens. The voltages applied to the skimmer and tube lens were 0 and 50 V, respectively. The applied RF voltages on the quadrupole and octapole were 400 V peak-to-peak. The gate lens regulating the ion injection into the ion-trap analyzer utilized an applied voltage of 16 V, whereas the voltage on the entrance lens for the eventual focusing of the transported ions was 30 V.

Results and discussion

(De)protonation

The positive- and negative-ion DART mass spectra of Asn (Mr 132) shown in Figure 1 are representative examples. The mass spectra show the dominant ion peaks of the (de)protonated analytes $[\text{Asn} \pm \text{H}]^{\pm}$, which are the major ion species commonly observed when ionizing various other amino acids. The ion species observed in the DART mass spectra of each of the amino acids are summarized in Table 1. The protonated analytes $[\text{M} + \text{H}]^+$ are most likely produced via proton transfer reactions involving $\text{H}_3\text{O}^+(\text{H}_2\text{O})_n$, the typical positive background ions in DART.⁴ Proton affinities of analytes M used⁸ are higher than that of H_2O ($691.0 \text{ kJ mol}^{-1}$)⁸ and its clusters $(\text{H}_2\text{O})_n$, as listed in Table 1.



The reactant ions $\text{H}_3\text{O}^+(\text{H}_2\text{O})_n$ can be formed via a Penning ionization to form $\text{H}_2\text{O}^{\cdot+}$ (reaction 2), due to the energy transfer from an excited He with 19.8 eV excitation energy, $\text{He}(2^3\text{S})$, to H_2O having an ionization energy of 12.6 eV, and subsequent reactions involving additional H_2O (reactions 3 and 4).

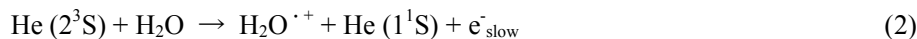
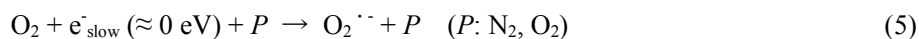
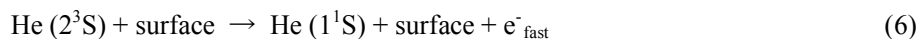


(Figure 1) and (Table 1)

In contrast, the formation of deprotonated analytes $[M - H]^-$ are most likely attributed to two different processes, i.e., proton transfer from analytes M to the negative background ions $O_2^{\cdot -}$ ⁵ and resonant electron capture by M . The $O_2^{\cdot -}$ ions are formed via attachment of thermal electrons having kinetic energies at the ambient temperature, i.e., e^-_{slow} (≈ 0 eV), to O_2 (reaction 5):



where P represents common air constituents such as N_2 and O_2 corresponding to a third body. Slow electrons e^-_{slow} with low kinetic energies can be produced via Penning ionization (reactions 2, 10 and 12) and/or the following surface Penning ionization (reaction 6).⁵



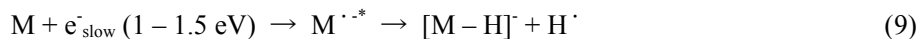
The electrons formed via reaction 6, e^-_{fast} , are rapidly thermalized by collisions with common air constituents P (reaction 7).



The collision of $O_2^{\cdot -}$ with analytes M efficiently brings about the formation of $[M - H]^-$ via proton transfer from M to $O_2^{\cdot -}$ (reaction 8), due to higher proton affinity of $O_2^{\cdot -}$ (1477 ± 2.9 kJ mol^{-1})¹⁵ rather than $[M - H]^-$.^{9,10}



The slow electrons having kinetic energies over the range of 1 – 1.5 eV, e^-_{slow} (1 – 1.5 eV), can also resonantly attach to analytes M and subsequent dehydrogenation leads to produce $[M - H]^-$ (reaction 9).



The formation of deprotonated amino acids $[M - H]^-$ via reaction 9 has been previously reported

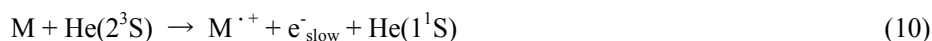
1
2
3
4
5
6 by numerous studies regarding resonant electron capture and dissociative electron attachment
7
8 using low energetic electrons.¹⁶⁻²⁰ On the basis of those previous studies, the $[M - H]^-$ ions
9
10 resulting from reaction 9 have carboxylate anion structures occurring via either electron capture
11
12 into the π^* orbital of the carboxylic group¹⁸ or hydrogen-atom tunneling through the barrier that
13
14 separates a dipole-supported minimum and repulsive valence state.¹⁹
15
16

17
18 In order to confirm whether both proton transfer with $O_2^{\cdot -}$ (reaction 8) and resonant
19
20 electron capture (reaction 9) are involved in deprotonation of various analytes in DART, some
21
22 analytes were ionized in the analyte ionization area under N_2 atmosphere conditions. It can be
23
24 expected that N_2 atmosphere conditions where few amounts of O_2 are present results in the
25
26 inhibition in occurrence of reaction 8 involving $O_2^{\cdot -}$. The mass spectra of Gly, Val, Asp and Phe,
27
28 arbitrary selected, obtained under N_2 atmosphere conditions certainly showed the ion peaks of
29
30 deprotonated analytes $[M - H]^-$ for individual analytes M, whose absolute abundances were
31
32 lower than those observed in normal ambient air conditions (Table S1 in Supplementary
33
34 Material). These results can evidence the involvement of both reactions 8 and 9 in deprotonation
35
36 occurring in DART.
37
38
39
40
41
42
43
44
45

46 47 ***Molecular ion formation***

48
49
50 Positive-ion DART brought about the formation of molecular cation $M^{\cdot +}$ for almost all the
51
52 analytes M whose abundances were quite lower than those of protonated analytes $[M + H]^+$, as
53
54 shown in Table 1. The $M^{\cdot +}$ formation has been reported in the previous studies of DART to
55
56
57
58
59
60

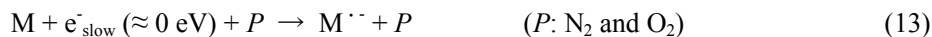
analyze nonpolar compounds such as dibenzosuberone and *n*-hexadecane.²¹ Taking into account the ionization energies of analytes M used, ≈ 9 eV (listed in Table 1),¹¹⁻¹³ and the previous report,²¹ $M^{\cdot+}$ can be formed via Penning ionization involving He(2^3S) (reaction 10) and/or charge transfer reaction from $O_2^{\cdot+}$ to M (reaction 11). The $O_2^{\cdot+}$ ion is one of the positive background ions produced via Penning ionization of O_2 having an ionization energy of 12.07 eV with He(2^3S) (reaction 12).²¹



In contrast, the formation of molecular anion $M^{\cdot-}$ in negative-ion DART of a given analyte M was investigated using the abundances of the ion peak whose m/z value corresponds to the molecular mass of M and the isotopes of deprotonated analyte $[M - H]^-$. The negative-ion mass spectrum of Asn (Figure 1b) shows the negative ion at m/z 132 with abundance of 12.0 % relative to deprotonated Asn $[\text{Asn} - H]^-$ (RA = 12.0 %). The ion at m/z 132 corresponds to not only molecular anion $\text{Asn}^{\cdot-}$ but also deprotonated Asn $[\text{Asn} - H]^-$ having one isotope of ^{13}C , ^2H , ^{17}O or ^{15}N . The calculated RA of the isotope of $[\text{Asn} - H]^-$ at m/z 132 is 5.3 %. That is, RA of $\text{Asn}^{\cdot-}$ formed in the negative-ion DART is 6.7 %. The other negative-ion mass spectra obtained (Figures 2, 3 and S1 – 16) indicated that Asp can be ionized as $\text{Asp}^{\cdot-}$ with RA of 14.6 %. In the case of Lys and Phe, the ions at m/z 146 and 165 corresponding to individual $M^{\cdot-}$ were detected at RAs of 6.2 and 6.8 %, respectively (Figures S9 and S13). Because the mass spectra of those analytes include the ion peaks that are higher in m/z values than $M^{\cdot-}$, the ions at m/z 146 and 165 may be the fragments from the ions with higher m/z values as well as $M^{\cdot-}$. High resolution

1
2
3
4
5
6 experiments with accurate mass measurement would be useful for further investigation of the
7
8 molecular anion formation for Lys and Phe.
9

10
11 The formation of $M^{\cdot-}$ of Asn and Asp has been previously observed under low-pressure
12 argon plasma conditions involving low energetic electrons.¹⁶ Taking into account the previous
13 report, molecular anion formation occurring in DART is attributable to resonant capture of
14 thermal electrons $e^-_{\text{slow}} (\approx 0 \text{ eV})$ by analytes M and simultaneous removal of excess energy in
15 $M^{\cdot-}$ by third bodies P such as N_2 and O_2 (reaction 13).
16
17
18
19
20
21



23
24 It has been previously reported that analytes M having dipole moments larger than the critical
25 magnitudes (2 – 2.5 Debye) are able to create so-called dipole-bound or dipole-supported
26 negative ion states and resulting in high efficiency in resonant electron capture.¹⁹ However, the
27 results obtained here, that Asn and Asp can more efficiently capture thermal electrons than other
28 amino acids, cannot be explained by the dipole moments individual amino acids in the global
29 minimum structures.¹⁴ For example, the dipole moment of Asp, 2.28 Debye, is equal to that of
30 Thr, which can inefficiently capture thermal electrons. In order to understand why Asn and Asp
31 have particularly high efficiency in resonant electron capture, further experimental and
32 theoretical studies will be required.
33
34
35
36
37
38
39
40
41
42
43
44
45
46
47
48
49
50
51

52 **Fragmentation**

53
54 Ionization Glu and Gln, acidic and amidic amino acids respectively, involved significant
55
56
57
58
59
60

1
2
3
4
5
6 fragmentation, in which the common neutral species are lost under positive- and negative-ion
7
8 modes and resulting in the formation of the fragment ions with RAs higher than about 10 %.
9
10 Figure 2 shows the positive- and negative-ion DART mass spectra of Glu (Mr 147). The mass
11
12 spectra include the ion peaks of not only the (de)protonated Glu $[\text{Glu} \pm \text{H}]^{\pm}$ but also fragment
13
14 ions corresponding to $[\text{Glu} \pm \text{H} - \text{H}_2\text{O}]^{\pm}$. It should be noted that in Figure 2, H_2O loss fragments
15
16 were observed in both positive- and negative-ion modes, indicative of the occurrence of H_2O
17
18 loss, independent of ionization. It is well-known that Glu easily forms pyroglutamic acid (PGA;
19
20 Mr 129) due to intramolecular thermal dehydration below $400\text{ }^{\circ}\text{C}$.²² Taking into account the
21
22 temperature of He gas flow used, $350\text{ }^{\circ}\text{C}$, the formation of $[\text{PGA} \pm \text{H}]^{\pm}$ (corresponding to $[\text{Glu} \pm$
23
24 $\text{H} - \text{H}_2\text{O}]^{\pm}$) in DART is most likely attributable to the following processes:

- 25
26
27
28
29
30 (a) Initial loss of H_2O from Glu to form PGA during the thermal desorption process in the He
31
32 gas stream (reaction 14)
33
34
35 (b) Subsequent formation of (de)protonated PGA $[\text{PGA} \pm \text{H}]^{\pm}$ via proton transfer reactions of
36
37 PGA with $\text{H}_3\text{O}^+(\text{H}_2\text{O})_n$ and O_2^- (reactions 15 and 16) and resonant electron capture by
38
39 PGA (reaction 17)
40
41

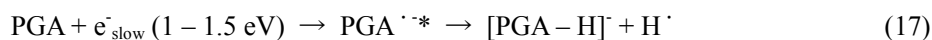
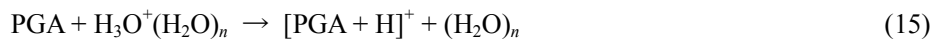
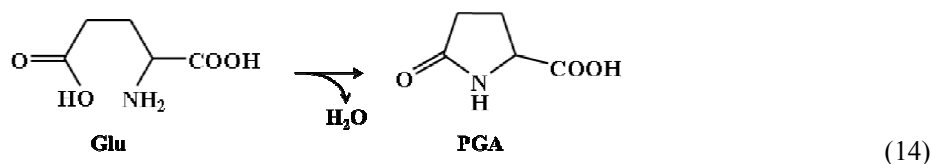
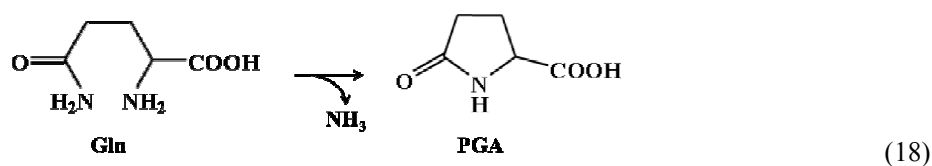


(Figure 2)

Ionization of Gln led to the fragment ions of (de)protonated Gln $[\text{Gln} \pm \text{H}]^{\pm}$ with NH_3 loss, $[\text{Gln} \pm \text{H} - \text{NH}_3]^{\pm}$, which have the same m/z values as $[\text{PGA} \pm \text{H}]^{\pm}$ corresponding to the fragment ions for Glu (Figure S8 Table 1). Taking into account the pyrolysis of Gln, it can be presumed that the fragmentation processes involved in DART ionization of Gln are similar to those of Glu described above. That is, Gln can initially cyclize to pyroglutamic acid (PGA) with loss of NH_3 during thermal desorption (reaction 18),²³ resulting in the formation of (de)protonated PGA $[\text{PGA} \pm \text{H}]^{\pm}$ via reactions 15 – 17.



DART of the other amino acids brought about the formation of some fragment ions, i.e., protonated Tyr with CO_2 loss $[\text{Tyr} + \text{H} - \text{CO}_2]^+$ (Figure 3), protonated Asp with H_2O loss $[\text{Asp} + \text{H} - \text{H}_2\text{O}]^+$ and deprotonated Asp with NH_3 loss $[\text{Asp} - \text{H} - \text{NH}_3]^-$ (Figure S10), whose RAs were lower than 10 %. Neutral species lost during the fragmentation in case of Tyr and Asp are changed with varying the polarity of ionization, which suggests that those fragmentations occur due to excess energy obtained via (de)protonation. The results obtained suggest, therefore, that the fragmentation occurring in DART is most likely attributable to both pyrolysis during thermal desorption and excess energy obtained via ionization reactions.

Oxidation

DART ionization resulted in the formation of (de)protonated analytes with the addition of one and/or two oxygens, $[M \pm H + nO]^{\pm}$ ($n = 1, 2$), for sulfur-containing, aromatic, and aromatic heterocyclic amino acids such as Met, Phe, Tyr, Trp and His (see Figure 3 and Table 1). It has been previously reported that these five amino acids can be easily oxidized with oxygen attachment due to hydroxyl radical HO^{\cdot} as a strong oxidizing species, formed in ozonated solutions²⁴⁻²⁶ or via Fenton reactions and/or radiolysis in aqueous solutions.²⁷ Scheme 1 shows oxygen addition products $[M + nO]$ of five amino acids M resulting from oxidation by HO^{\cdot} , on the basis of the previous reports.²⁵⁻²⁷ The oxidation of Met with HO^{\cdot} results in the formation of sulfoxide²⁵⁻²⁷ (Scheme 1a). Reactions of HO^{\cdot} with the aromatic rings in Phe and Tyr lead to the addition of HO^{\cdot} to the rings, and subsequent reactions of the radical species with oxygen generate 2-amino-3-(hydroxyphenyl)propanoic acid²⁷ and dihydroxyphenylalanine,^{25,27} corresponding to the monoxides of Phe and Tyr, respectively (Schemes 1b and c). It has been reported that aromatic amino acids are oxidized to form quinones, e.g., 2-amino-3-(3,4-dioxo-cyclohexa-1,5-dienyl)-propanoic acid which is a quinone structural oxidation product for Tyr.²⁶ However, no observation of ions related to quinones in the mass spectra of Phe and Tyr (Figures S13 and 3) indicates less occurrence of quinone formation in DART. Trp and His can be oxidized at the conjugated double bond moiety with HO^{\cdot} to form oxindole-3-alanine ($[Trp + O]$), *N*-formylkynurenine ($[Trp + 2O]$) and 2-oxo-histidine ($[His + O]$) (Schemes 1d and e). The oxidation reactivity for individual amino acids M can be estimated using relative abundances of $[M \pm H + nO]^{\pm}$ listed in Table 1. The reactivity order obtained here

1
2
3
4
5
6 is Trp > Met > Phe > Tyr > His > other amino acids \approx 0. This order is in agreement with that
7
8 reported by Kotiaho *et al.* using ozonated solutions with pH 5.8: Met > Trp > Tyr > His > other
9
10 amino acids.²⁵ In the case of higher pH conditions, oxidation of Cys to form trioxide products
11
12 [Cys + 3O] proceeds most dominantly.^{24,28} Taking into account the results obtained, the
13
14 oxidation with oxygen attachment reactions occurring in DART most likely originate with HO \cdot
15
16
17
18 in the ionization area under relatively acidic conditions.
19
20
21
22

23 **(Figure 3) and (Scheme 1)**
24
25
26
27
28
29

30 ***Hydrogen loss***

31
32

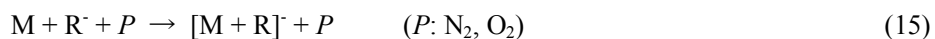
33 In negative-ion DART, deprotonated analytes with two hydrogen loss, [M – 2H – H] $^-$, were
34
35 observed when analyzing Gly, Ala, Val, Leu, Ile, Ser, Thr, Asn, Cys, Met and Phe, which have
36
37 aliphatic or non-ionic side chains (see Figure 1 and Table 1). The peak abundances from [M –
38
39 2H – H] $^-$ were rather low compared to the abundances of [M – H] $^-$. Such [M – 2H – H] $^-$ ions
40
41 have also been observed in the negative-ion DART of aliphatic compounds such as hexanes,
42
43 heptanes, cyclohexane²⁹ and hexatriacontane⁷, although the precise mechanism of the 2H loss
44
45 reactions in DART and its dependence on the structural properties of the analytes have not yet
46
47 been clarified. It has been previously reported that deprotonated Ser in aqueous solution with
48
49 HO \cdot and O₂ loses two hydrogens from the backbone of Ser via sequential oxidation reactions,
50
51 as shown in Scheme 2.³⁰ This scheme could be applied to the reactions observed here, i.e., the
52
53
54
55
56
57
58
59
60

1
2
3
4
5
6 gas-phase 2H loss from deprotonated analytes for various amino acids including Ser. In contrast,
7
8 the ion peaks of $[M - 2H - H]^-$ have been observed in the mass spectra of Gly and Val
9
10 resonantly capturing low energetic electrons (≈ 1.5 eV).^{17,20} It is likely, therefore, that the 2H
11
12 loss reactions occurring in DART can be interpreted in terms of alternative oxidation processes
13
14 due to HO^\cdot and/or involvement of slow electrons e^-_{slow} (≈ 1.5 eV) formed via reactions 2, 7, 10
15
16 and 12.
17
18
19
20
21
22

23 (Scheme 2)

24 25 26 27 28 29 30 **Formation of adducts with negative background ions**

31
32
33 All of the amino acids M, except for acidic and amidic amino acids such as Asp, Glu and
34
35 Gln, formed negative ion adducts $[M + R]^-$ with background ions R^- , such as O_2^- (m/z 32),
36
37 HCO_2^- (m/z 45), NO_2^- (m/z 46) and/or $COO^-(COOH)$ (m/z 89). Those ions R^- are typical
38
39 negative backgrounds formed in DART. The $COO^-(COOH)$ ion can be observed in the
40
41 negative-ion mass spectra of Tyr (Figure 3b), whereas O_2^- and NO_2^- are included in a DART
42
43 mass spectrum of negative background ions reported by Cody *et al.*⁷ The adduct ions $[M + R]^-$
44
45 were most likely formed via three-body reactions with a third body P such as N_2 or O_2 .
46
47
48



50
51
52 The adduct ions $[M + R]^-$ observed are summarized in Table 1. Table 1 shows that whether $[M +$
53
54 $R]^-$ are formed or not varies with each combination of R^- and M, which are not dependent upon
55
56
57
58
59
60

1
2
3
4
5
6 the chemical properties of M, such as whether the analyte is aliphatic or aromatic, or has certain
7
8 functional groups. The results obtained suggest that the formation of the $[M + R]^-$ adducts is
9
10 attributed to the affinity or ability of complexation between individual R^- and M, although the
11
12 factors determining its affinity or ability can not be readily proven. The similar phenomena have
13
14 been also observed in atmospheric pressure corona discharge ionization (APCDI).^{31,32}
15
16
17
18
19
20
21
22

23 ***Ionization characteristics of DART***

24
25
26 The notable reactions observed in DART were oxidations involving oxygen attachment and
27
28 hydrogen loss. As described above, those oxidation processes in DART are most likely
29
30 attributable to reactions with HO^\cdot . It can be presumed, therefore, that the analyte ionization area
31
32 between the DART source exit and the mass spectrometer orifice includes a number of active
33
34 oxygens such as HO^\cdot . This hypothesis is supported by the appearance of HCO_2^- , HCO_4^- and
35
36 $COO^-(COOH)$ as typical negative background ions. It has been found in previous studies of
37
38 kinetics and atmospheric pressure DC negative corona discharges that the formation of HCO_2^- ,
39
40 HCO_4^- and $COO^-(COOH)$ in the discharge area is attributable to discharge byproducts such as
41
42 O_3 and HO^\cdot , as well as CO originating from electrons having energy between 5 and 10 eV.^{31,33}
43
44
45
46
47 Taking those previous studies into account, Figure 4 shows the proposed sequential reactions for
48
49 the formation of O_3 , HO^\cdot , CO and the resulting negative background ions in DART involved
50
51 excited He, $He(2^3S)$ having 19.8 eV, as an energy source. The elementary processes shown in
52
53
54
55 Figure 4 are summarized in Table 2. Collisions of $He(2^3S)$ with O_2 can occur homolytically and
56
57
58
59
60

1
2
3
4
5
6 heterolytically in terms of bond dissociation to form an O atom in a ground-level triplet state,
7
8 $O(^3P)$, and the O^- ion, respectively (reactions a and e in Figure 4).³⁴ The oxygen atom $O(^3P)$ can
9
10 combine rapidly with O_2 to generate ozone O_3 (reaction b in Figure 4),³⁴ whereas O^- ion reacts
11
12 with H_2O resulting in the formation of HO^- ion (reaction f in Figure 4).³⁵ The reaction of HO^-
13
14 with O_3 brings about the formation of HCO_4^- via HO_2^- as an intermediate further reacting with
15
16 CO_2 (reactions h and i in Figure 4).^{26,36} It has been reported that O_3 molecules can dissociate
17
18 with an energy above 3.87 eV to produce an O atom in an excited singlet state, $O(^1D)$,³⁴ which
19
20 is likely achieved involving $He(2^3S)$ (reaction c in Figure 4). Subsequent reaction of $O(^1D)$ with
21
22 H_2O leads to the formation of HO^\cdot (reaction d in Figure 4).³⁴ The radical species HO^\cdot can also
23
24 be formed via reactions forming HO^- and H_3O^+ (reactions f and r in Figure 4).^{35,4} The formation
25
26 of $COO^\cdot(COOH)$ and HCO_2^- most likely originates from an association reaction of HO^\cdot with
27
28 CO (reaction j in Figure 4).³⁷ The CO can occur via the dissociation of CO_2 with an energy
29
30 above 8.3 eV (reaction t in Figure 4).⁴¹ It is most likely that the sequential reactions shown in
31
32 Figure 4 can occur inside a DART source, and the resulting HO^\cdot are introduced into the analyte
33
34 ionization area by the He gas flow, independent of the polarity of the voltage applied to the grid
35
36 electrode of the DART source exit. Therefore, the oxidation reactions due to HO^\cdot can occur
37
38 easily in both positive- and negative-ion modes.
39
40
41
42
43
44
45
46
47
48

49 **(Figure 4) and (Table 2)**
50
51
52
53

54 Based on these results, the ionization characteristics in DART can be summarized as
55
56 follows. The thermal desorption of condensed-phase analytes, $M_{(solid)}$, results in the formation of
57
58
59
60

1
2
3
4
5
6 gas-phase analytes, $M_{(\text{gas})}$, and fragments $[M - m]_{(\text{gas})}$ due to pyrolysis. The resulting gaseous
7
8 species $M_{(\text{gas})}$ and $[M - m]_{(\text{gas})}$ are ionized as $[M \pm H]^{\pm}$ and $[M - m \pm H]^{\pm}$ via (de)protonation
9
10 reactions involving the typical background ions $\text{H}_3\text{O}^+(\text{H}_2\text{O})_n$ and $\text{O}_2^{\cdot\cdot}$ and slow electrons (1 –
11
12 1.5 eV). Deprotonated analytes $[M \pm H]^{\pm}$ having excess energies can occur fragmentation with
13
14 loss of neutral species m to form $[M - m \pm H]^{\pm}$. The species $M_{(\text{gas})}$ can also react with $\text{He}(2^3\text{S})$,
15
16 $\text{O}_2^{\cdot+}$ and thermal electrons (≈ 0 eV) and several negative background ions R^- ($\text{O}_2^{\cdot-}$, HCO_2^- , NO_2^-
17
18 and $\text{COO}^-(\text{COOH})$) to product molecular ions $M^{\cdot\pm}$ and adduct ions $[M + \text{R}]^-$, respectively. In
19
20 contrast, the analytes which tend to be oxidized by HO^\cdot can be ionized as (de)protonated
21
22 analytes with O attachment and/or 2H loss, i.e., $[M + n\text{O} \pm H]^{\pm}$ and/or $[M - 2\text{H} - H]^-$. The
23
24 ionization processes occurring in DART and the resulting product ion species are shown in
25
26 Figure 5.
27
28
29
30
31
32
33
34

35 **(Figure 5)**
36
37
38
39
40
41

42 **Conclusions**

43
44
45 The positive and negative ionization characteristics of 20 different α -amino acids were
46
47 investigated in Direct Analysis in Real Time (DART) mass spectrometry. All of the amino acids
48
49 except for Arg were ionized via various reactions depending on the physicochemical and/or
50
51 structural properties of the individual amino acids, as follows:
52
53
54

- 55 1) (De)protonation for almost all of amino acids except for Arg via proton transfer
56
57
58
59
60

1
2
3
4
5
6 reactions with the typical background ions $\text{H}_3\text{O}^+(\text{H}_2\text{O})_n$ and $\text{O}_2^{\cdot\cdot}$ and resonant electron
7
8 capture by M.
9

- 10 2) Molecular cation formation for almost all of amino acids except for Arg.
- 11
- 12 3) Molecular anion formation for the specific amino acids such as Asn and Asp.
- 13
- 14
- 15 4) Pyrolysis for Glu and Gln.
- 16
- 17
- 18 5) Fragmentation for Tyr and Asp due to excess energy obtained via ionization reactions.
- 19
- 20 6) Oxygen attachment for sulfur-containing, aromatic and aromatic heterocyclic amino
- 21 acids.
- 22
- 23
- 24
- 25 7) Hydrogen loss for aliphatic or non-ionic amino acids.
- 26
- 27
- 28 8) Attachment of negative background ions R^- ($\text{O}_2^{\cdot\cdot}$, HCO_2^- , NO_2^- and $\text{COO}^-(\text{COOH})$) for
29 almost all of the amino acids to form $[\text{M} + \text{R}]^-$.
- 30
- 31

32 Oxygen attachment and hydrogen loss can be interpreted as oxidation processes involving
33 active oxygens such as hydroxyl radical HO^\cdot . The results suggest, therefore, that analyte
34 ionization in DART can be oxidatively influenced by HO^\cdot .
35
36
37
38
39
40
41
42

43 **Acknowledgments**

44
45
46 This work was supported by Grants-in-Aid for Scientific Research (C) (23550101 and
47 24619005) from the Ministry of Education, Culture, Sports, Science and Technology of Japan.
48
49
50
51
52
53
54
55
56
57
58
59
60

References

1. S. Soparawalla, G. A. Salazar, R. H. Perry, M. Nicholas, R. G. Cooks, *Rapid Commun. Mass Spectrom.*, 2009, **23**, 131-137.
2. R. R. Steiner, R. L. Larson, *J. Forensic Sci.*, 2009, **54**, 617-622.
3. C. Petucci, J. Diffendal, D. Kaufman, B. Mekonnen, G. Terefenko, B. Mussleman, *Anal. Chem.*, 2007, **79**, 5064-5070.
4. R. B. Cody, J. A. Laramée, H. D. Durst, *Anal. Chem.*, 2005, **77**, 2297-2302.
5. E. S. Chernetsova, G. E. Morlock, I. A. Revelsky, *Russ. Chem. Rev.*, 2011, **80**, 235-255.
6. R. B. Cody, *Anal. Chem.*, 2009, **81**, 1101-1107.
7. R. B. Cody, A. J. Dane, *J. Am. Soc. Mass Spectrom.*, 2013, **24**, 329-334.
8. E. P. Hunter, S. G. Lias, *J. Phys. Chem. Ref. Data*, 1998, **27**, 413-656.
9. C. M. Jones, M. Bernier, E. Carson, K. E. Colyer, R. Metz, A. Pawlow, E. D. Wischow, I. Webb, E. J. Andriole, J. C. Poutma, *Int. J. Mass Spectrom.*, 2007, **267**, 54-62.
10. R. J. O'Hair, J. M. Bowie, S. Gronert, *Int. J. Mass Spectrom. Ion Proc.*, 1992, **117**, 23-36.
11. P. H. Cannington, N. S. Ham, *J. Electron Spectrosc. Relat. Phenon.*, 1983, **32**, 139-151.
12. L. Klasinc, *J. Electron Spectrosc. Relat. Phenon.*, 1976, **8**, 161-164.
13. M. A. Slifkin, A. C. Allison, *Nature*, 1967, **215**, 949-
14. K. Koyanagi, Y. Kita, M. Tachikawa, *Eur. Phys. J. D*, 2012, **66**, 121.
15. M. J. Travers, D. C. Cowles, G. B. Ellison, *Chem. Phys. Lett.*, 1989, **164**, 449-455.
16. D. Voigt, J. Schmidt, *Biomed. Mass Spectrom.*, 1978, **5**, 44-46.
17. Y. V. Vasil'ev, B. J. Figard, V. G. Voinov, D. F. Barofsky, M. L. Deinzer, *J. Am. Chem. Soc.*,

- 2006, **128**, 5506-5515.
18. A. M. Scheer, P. Mozejko, G. A. Gallup, P. D. Burrow, *J. Chem. Phys.*, 2007, **126**, 174301.
19. Y. V. Vasil'ev, B. J. Figard, D. F. Barofsky, M. L. Deinzer, *Int. J. Mass Spectrom.*, 2007, **268**, 106-121.
20. S. Denifl, H. D. Flosadóttir, A. Edtbauer, O. Ingólfsson, T. D. Márk, P. Scheier, *Eur. Phys. J. D*, 2010, **60**, 37-44.
21. R. B. Cody, *Anal. Chem.*, 2009, **81**, 1101-1107.
22. J. Douda, V. A. Basiuk, *J. Anal. Appl. Pyrolysis*, 2000, **56**, 113-121.
23. W. M. Lagna, P. S. Callery, *Biomedical Mass Spectrom.*, 1985, **12**, 699-703.
24. J. B. Mudd, R. Leavitt, A. Ongun, T. T. McManus, *Atmos. Environ.*, 1969, **3**, 669-682.
25. T. Kotiaho, M. N. Eberlin, P. Vainiotalo, R. Kostianen, *J. Am. Soc. Mass Spectrom.*, 2000, **11**, 526-535.
26. V. K. Sharma, N. J. D. Graham, *Ozone: Science & Engineering*, 2010, **32**, 81-90.
27. K. Takamoto, M. R. Chance, *Annu. Rev. Biophys. Biomol. Struct.*, 2006, **35**, 251-276.
28. W. A. Pryor, D. H. Giamalva, D. F. Church, *J. Am. Chem. Soc.*, 1984, **106**, 7094-7100.
29. L. Song, A. B. Dykstra, H. Yao, J. E. Bartmess, *J. Am. Soc. Mass Spectrom.*, 2009, **20**, 42-50.
30. R. M. Le Lacheur, W. H. Graze, *Environ. Sci. Technol.*, 1996, **30**, 1072-1080.
31. K. Sekimoto, M. Sakai, M. Takayama, *J. Am. Soc. Mass Spectrom.*, 2012, **23**, 1109-1119.
32. K. Sekimoto, N. Matsuda, M. Takayama, *Mass Spectrometry*, 2013, **2**, A0020.
33. K. Sekimoto, M. Takayama, *Eur. Phys. J. D*, 2010, **60**, 589-599.
34. D. J. Jacob, *Introduction to Atmospheric Chemistry*, 1st edn., pp. 163-171, Princeton

1
2
3
4
5
6 University Press, Princeton, New Jersey (1999).
7

8 35. F. C. Fehsenfeld, E. E. Ferguson, *J. Chem. Phys.*, 1974, **61**, 3181-3193.
9

10 36. T. McAllister, A. J. C. Nicholson, D. L. Swingler, *Int. J. Mass Spectrom. Ion Phys.*, 1978,
11
12 **27**, 43-48.
13

14 37. B. J. Finlayson-Pitts, J. N. Pitts Jr., *Chemistry of the Upper and Lower Atmosphere*, 1st edn.,
15
16 pp. 137-138. Academic Press, San Diego (2000).
17

18 38. N. Getoff, *Int. J. Hydrogen Energ.*, 1994, **19**, 667-672.
19

20 39. J. L. Pack, A. V. Phelps, *J. Chem. Phys.*, 1966, **44**, 1870-1883.
21

22 40. L. M. Chanin, A. V. Phelps, M. A. Bionidi, *Phys. Rev.*, 1962, **128**, 219-230.
23

24 41. D. R. Lide, *Handbook of Chemistry and Physics*, 88th edn., pp. 9-56, CRC Press, Boca
25
26 Raton (2007).
27
28
29
30
31
32
33
34
35
36
37
38
39
40
41
42
43
44
45
46
47
48
49
50
51
52
53
54
55
56
57
58
59
60

Legends of Figures, Tables and Schemes

Figure 1. (a) Positive- and (b) negative-ion DART mass spectra of L-asparagine (Asn). A_{BP} represents the absolute abundance (arbitrary units) of the base peak in each mass spectrum.

Figure 2. (a) Positive- and (b) negative-ion DART mass spectra of L-glutamic acid (Glu). A_{BP} represents the absolute abundance (arbitrary units) of the base peak in each mass spectrum.

Figure 3. (a) Positive- and (b) negative-ion DART mass spectra of L-tyrosine (Tyr). A_{BP} represents the absolute abundance (arbitrary units) of the base peak in each mass spectrum.

Figure 4. Proposed sequential reactions for the formation of O_3 , OH^\cdot , CO and background ions such as $H_3O^+(H_2O)_n$, $O_2^{\cdot-}$, HCO_2^\cdot , HCO_4^\cdot and $COO^\cdot(COOH)$ in DART using He gas.

Figure 5. Summary of the ionization behavior in DART.

Table 1. Ion species and their relative abundances observed in the DART mass spectra of individual amino acids (Figures 1-3 and S1-16).

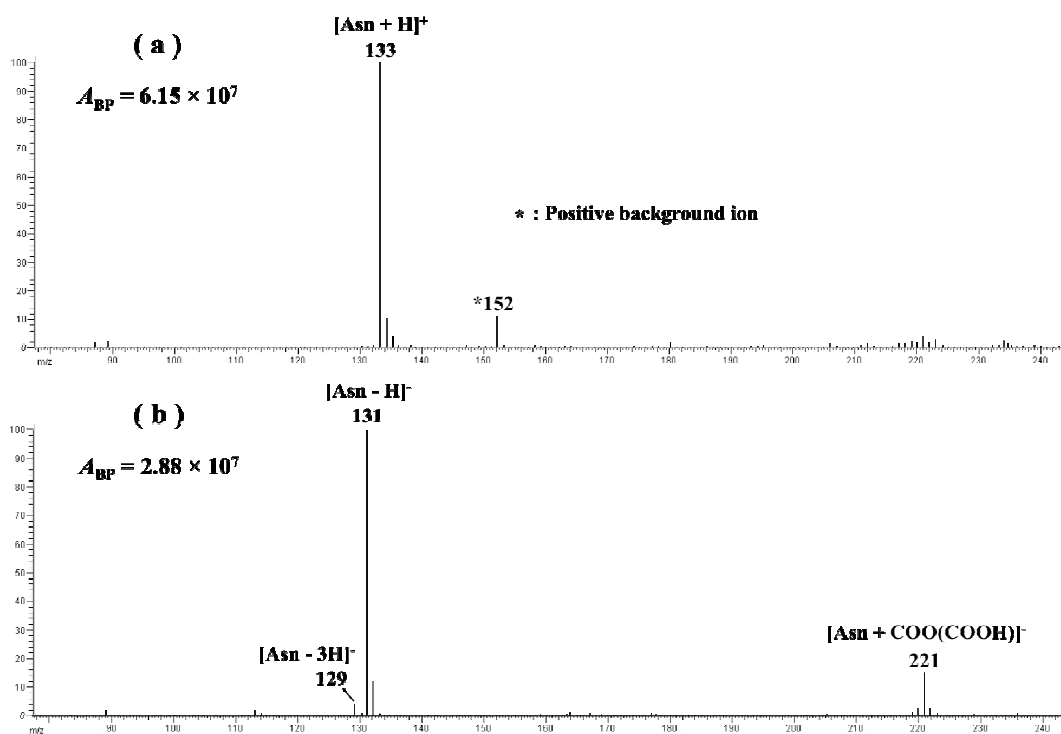
1
2
3
4
5
6
7
8 Table 2. Elementary processes for the formation of O_3 , OH^\cdot , CO and background ions including

9
10 $H_3O^+(H_2O)_n$, O_2^- , HCO_2^- , HCO_4^- and $COO^-(COOH)$ in DART using He gas.

11
12
13
14
15 Scheme 1. Oxygen addition products of (a) methionine (Met), (b) phenylalanine (Phe), (c)

16
17 tyrosine (Tyr), (d) tryptophane (Trp) and (e) histidine (His).

18
19
20
21
22 Scheme 2. Reaction of deprotonated amino acids with HO^\cdot and O_2 to lose two hydrogens.



34 **Figure 1. (a) Positive- and (b) negative-ion DART mass spectra of L-asparagine (Asn). A_{BP}**
35 **represents the absolute abundance (arbitrary units) of the base peak in each mass**
36 **spectrum.**

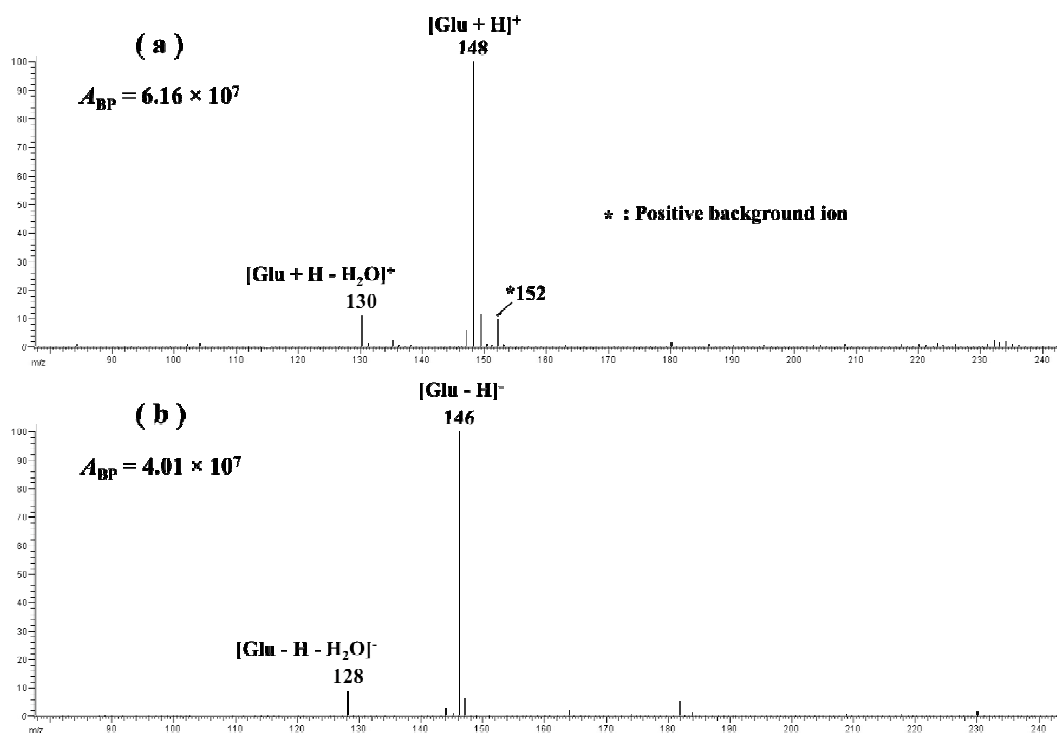


Figure 2. (a) Positive- and (b) negative-ion DART mass spectra of L-glutamic acid (Glu).

A_{BP} represents the absolute abundance (arbitrary units) of the base peak in each mass spectrum.

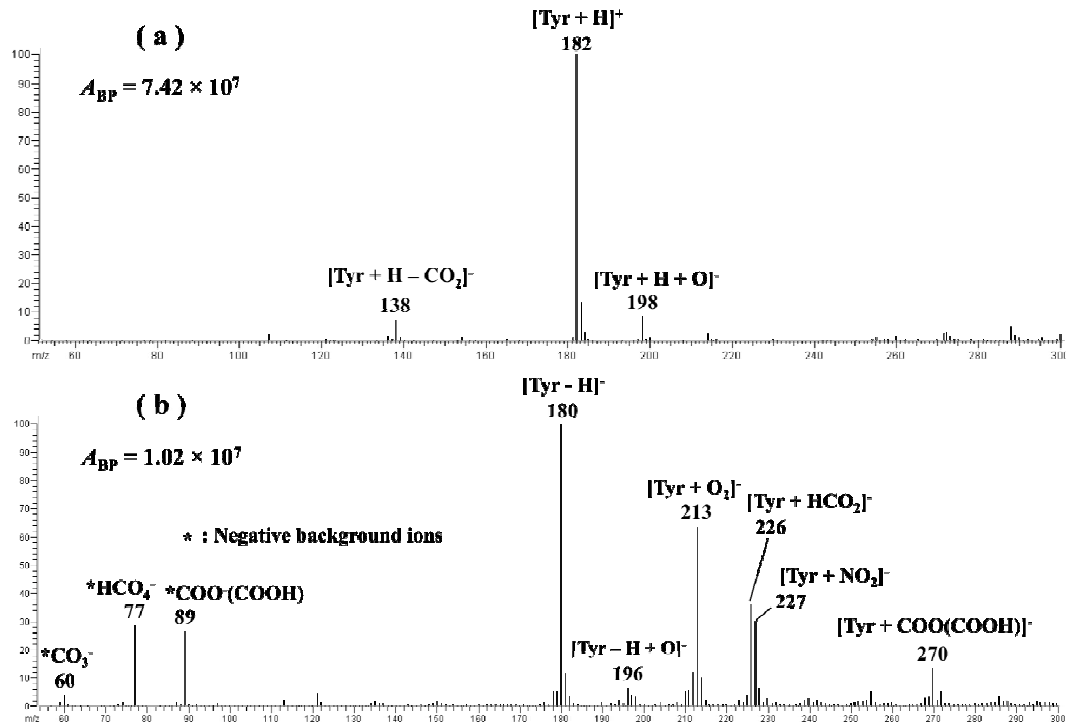


Figure 3. (a) Positive- and (b) negative-ion DART mass spectra of L-tyrosine (Tyr). A_{BP} represents the absolute abundance (arbitrary units) of the base peak in each mass spectrum.

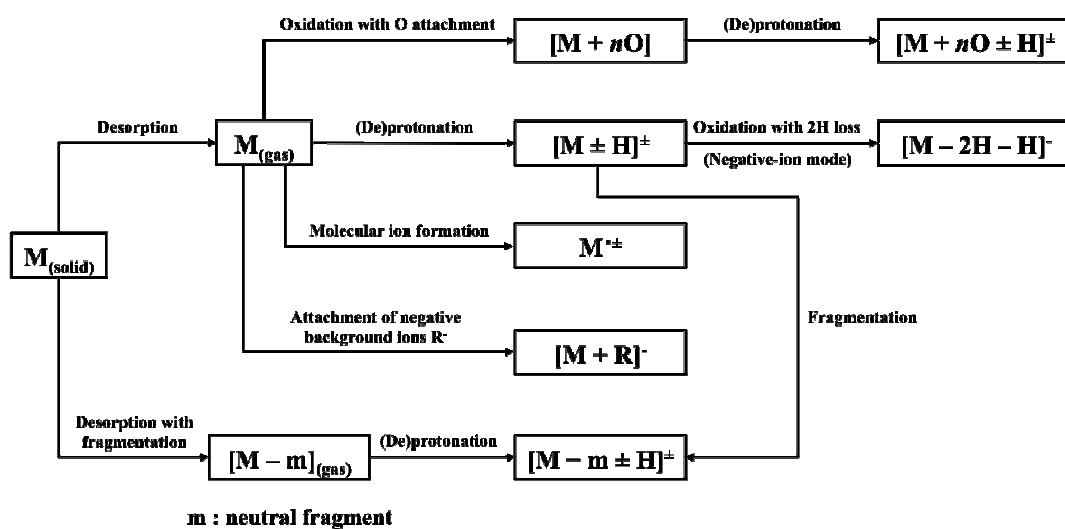


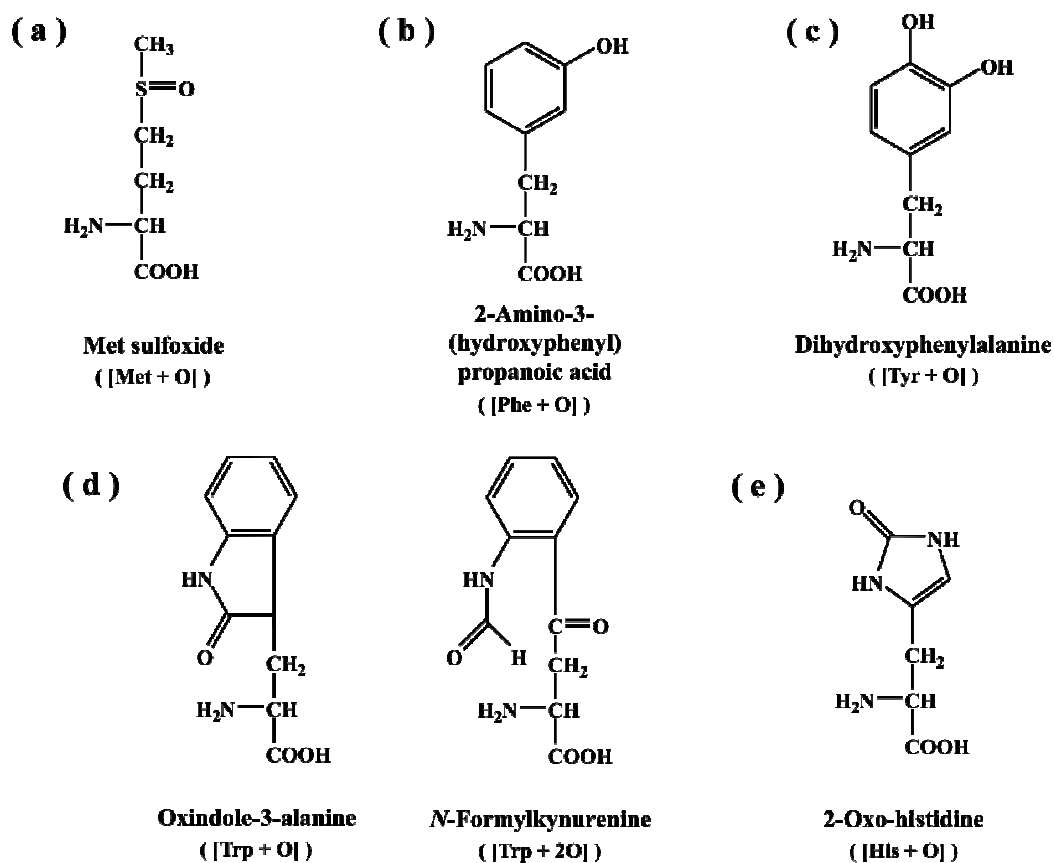
Figure 5. Summary of the ionization behavior in DART.

Table 2. Elementary processes for the formation of O₃, OH[·], CO and background ions including H₃O⁺(H₂O)_{*n*}, O₂⁻, HCO₂⁻, HCO₄⁻ and COO⁻(COOH) in DART using He gas.

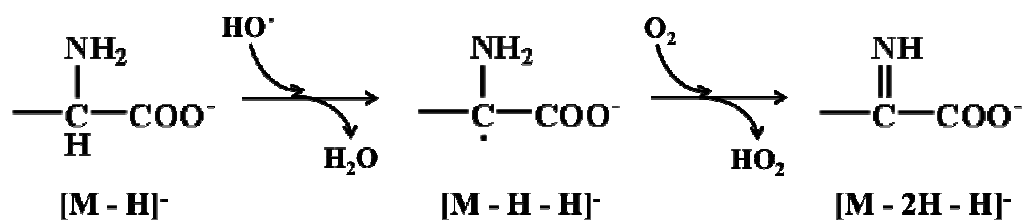
	Reaction	References
a	$O_2 + He(2^3S) \rightarrow O(^3P) + O(^1D) + He(1^1S)$	34
b	$O(^3P) + O_2 + P \rightarrow O_3 + P$	34
c	$O_3 + He(2^3S) \rightarrow O(^1D) + O_2^{-\cdot} + e^{-}_{slow} + He(1^1S)$	-
d	$O(^1D) + H_2O \rightarrow 2HO^{\cdot}$	34
e	$O_2 + He(2^3S) \rightarrow O^{\cdot-} + O^{\cdot} + He(1^1S)$	-
f	$O^{\cdot} + H_2O \rightarrow HO^{\cdot} + HO^{\cdot}$	35
g	$HO^{\cdot} + e^{-}_{slow} + P \rightarrow HO^{\cdot} + P$	-
h	$HO^{\cdot} + O_3 \rightarrow HO_2^{\cdot} + O_2$	26
i	$HO_2^{\cdot} + CO_2 + P \rightarrow HCO_4^{\cdot-} + P$	36
j-1	$HO^{\cdot} + CO \rightarrow COOH$	37
j-2	$2COOH \rightarrow (COOH)_2$	37
k	$(COOH)_2 \rightarrow HCOOH + CO_2$	37, 38
l	$(COOH)_2 + A^{\cdot-} \rightarrow COO^{\cdot-}(COOH) + HA$	-
m	$HCOOH + A^{\cdot-} \rightarrow HCO_2^{\cdot-} + HA$	-
n	$O_2 + e^{-}_{slow} + P \rightarrow O_2^{-\cdot} + P$	39, 40
o-1	$surface + He(2^3S) \rightarrow surface + e^{-}_{fast} + He(1^1S)$	4
o-2	$e^{-}_{fast} + P \rightarrow e^{-}_{low} + P$	-
p	$H_2O + He(2^3S) \rightarrow H_2O^{\cdot+} + e^{-}_{slow} + He(1^1S)$	4
q	$H_2O^{\cdot+} + H_2O \rightarrow H_3O^{\cdot+} + HO^{\cdot}$	4
r	$H_3O^{\cdot+} + (H_2O)_n \rightarrow H_3O^{\cdot+}(H_2O)_n$	4
s	$CO_2 + He(2^3S) \rightarrow CO + O + He(1^1S)$	41

P: third body (N₂ and O₂)

A⁻: Negative ion which has a higher proton affinity than COO⁻(COOH) and HCO₂⁻



Scheme 1. Oxygen addition products of (a) methionine (Met), (b) phenylalanine (Phe), (c) tyrosine (Tyr), (d) tryptophane (Trp) and (e) histidine (His).



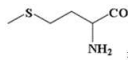
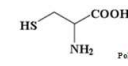
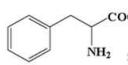
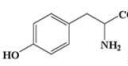
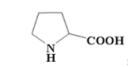
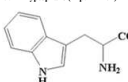
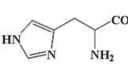
Scheme 2. Reaction of deprotonated amino acids with HO[•] and O₂ to lose two hydrogens.

Table 1. Ion species and their relative abundances observed in the DART mass spectra of individual amino acids (Figures 1-3 and S1-16).

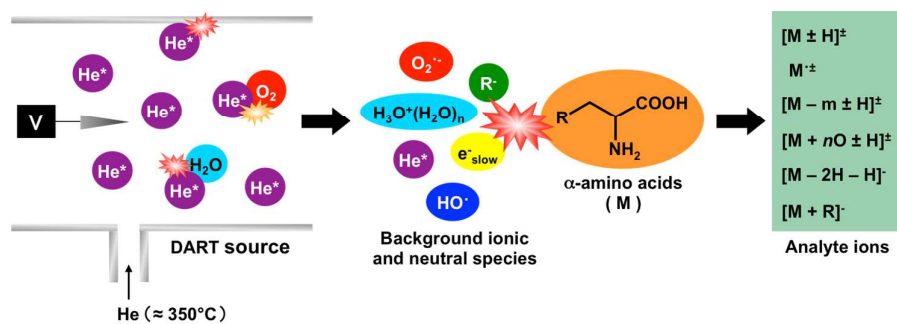
Amino acid (No)	Proton affinity of M and [M-H] ⁻ (kJ mol ⁻¹)	Ionization energy (eV)	Dipole moment ¹⁴ (Debye)	Ionization reaction	Positive ions (relative abundances [%])					Negative ions (relative abundances [%])					Attachment of negative background ions R ¹⁶			
					Protonation	Molecular cation formation	Fragmentation	Oxidation	Deprotonation	Molecular anion formation	Fragmentation	Oxidation	Hydrogen loss	R ¹⁶	O ₂	BCl ₃	NO ₂	COO(-COOH)
1. Glycine (Gly; Mr 75)	986.5 ^a 1416.0 ± 5.2 ^a	8.9 ¹⁰	1.33	[M + H] ⁺ (100)	M ⁺ (2.8)	-	-	-	[M - H] ⁻ (100)	-	-	-	[M - 2H - H] ⁻ (20.6)	[M + O ₂] ⁻ (2.5)	-	-	[M + COO(-COOH)] ⁻ (14.6)	
2. L-Alanine (Ala; Mr 89)	981.6 ^a 1420.0 ± 7.3 ^a	8.9	1.40	[M + H] ⁺ (100)	M ⁺ (2.4)	-	-	-	[M - H] ⁻ (100)	-	-	-	[M - 2H - H] ⁻ (33.0)	[M + O ₂] ⁻ (2.7)	[M + BCl ₃] ⁻ (2.5)	-	[M + COO(-COOH)] ⁻ (25.5)	
3. L-Valine (Val; Mr 117)	910.6 ^a 1420.0 ± 13.0 ^a	8.7 ¹⁰	1.40	[M + H] ⁺ (100)	M ⁺ (1.7)	-	-	-	[M - H] ⁻ (100)	-	-	-	[M - 2H - H] ⁻ (12.7)	[M + O ₂] ⁻ (3.6)	[M + BCl ₃] ⁻ (5.2)	[M + NO ₂] ⁻ (2.7)	[M + COO(-COOH)] ⁻ (17.2)	
4. L-Leucine (Leu; Mr 133)	914.6 ^a 1418.0 ± 12.0 ^a	8.5 ¹⁰	1.20	[M + H] ⁺ (100)	M ⁺ (2.4)	-	-	-	[M - H] ⁻ (100)	-	-	-	[M - 2H - H] ⁻ (24.5)	[M + O ₂] ⁻ (17.4)	[M + BCl ₃] ⁻ (13.9)	[M + NO ₂] ⁻ (5.1)	[M + COO(-COOH)] ⁻ (43.7)	
5. L-Isoleucine (Ile; Mr 133)	917.4 ^a 1417.0 ± 13.0 ^a	8.7 ¹⁰	1.36	[M + H] ⁺ (100)	M ⁺ (1.9)	-	-	-	[M - H] ⁻ (100)	-	-	-	[M - 2H - H] ⁻ (26.6)	[M + O ₂] ⁻ (19.7)	[M + BCl ₃] ⁻ (9.7)	[M + NO ₂] ⁻ (5.8)	[M + COO(-COOH)] ⁻ (27.6)	
6. L-Serine (Ser; Mr 105)	914.5 ^a 1392.0 ± 12.0 ^a	8.7 ¹⁰	1.96	[M + H] ⁺ (100)	M ⁺ (1.2)	-	-	-	[M - H] ⁻ (100)	-	-	-	[M - 2H - H] ⁻ (5.8)	[M + O ₂] ⁻ (1.2)	-	-	[M + COO(-COOH)] ⁻ (5.2)	
7. L-Threonine (Thr; Mr 119)	922.5 ^a 1389.0 ± 12.0 ^a	≤ 10.2 ¹⁰	2.28	[M + H] ⁺ (100)	M ⁺ (1.8)	-	-	-	[M - H] ⁻ (100)	-	-	-	[M - 2H - H] ⁻ (16.6)	[M + O ₂] ⁻ (2.5)	-	-	[M + COO(-COOH)] ⁻ (6.6)	
8. L-Asparagine (Asn; Mr 132)	929.9 ^a 1387.0 ± 13.0 ^a	-	2.93	[M + H] ⁺ (100)	M ⁺ (1.4)	[M + H - H ₂ O] ⁺ (3.7)	-	-	[M - H] ⁻ (100)	M ⁻ (6.7)	[M - H - NH ₂] ⁻ (9.2)	-	[M - 2H - H] ⁻ (4.6)	-	-	-	[M + COO(-COOH)] ⁻ (14.9)	
9. L-Glutamine (Gln; Mr 146)	927.8 ^a 1387.0 ± 13.0 ^a	-	3.44	[M + H] ⁺ (100)	M ⁺ (2.4)	[M + H - NH ₂] ⁺ (PGA-H) ⁺ (21.8)	-	-	[M - H] ⁻ (100)	M ⁻ (6.7)	[M - H - NH ₂] ⁻ (PGA-H) ⁻ (100)	-	-	-	-	-	-	
10. L-Lysine (Lys; Mr 146)	906.8 ^a 1411.0 ± 13.0 ^a	8.4 ¹⁰	2.43	[M + H] ⁺ (100)	M ⁺ (1.2)	-	-	-	[M - H] ⁻ (100)	M ⁻ (6.2)	-	-	-	[M + O ₂] ⁻ (9.2)	[M + BCl ₃] ⁻ (24.2)	[M + NO ₂] ⁻ (25.0)	[M + COO(-COOH)] ⁻ (26.8)	
11. L-Asparagine (Arg; Mr 176)	919.9 ^a 1386.0 ± 12.0 ^a	-	2.28	-	-	-	-	-	-	-	-	-	-	-	-	-	-	
12. L-Aspartic acid (Asp; Mr 133)	908.9 ^a -	-	2.28	[M + H] ⁺ (100)	M ⁺ (2.4)	-	-	-	[M - H] ⁻ (100)	M ⁻ (14.6)	-	-	-	-	-	-	-	
13. L-Glutamic acid (Glu; Mr 147)	913.9 ^a -	-	1.80	[M + H] ⁺ (100)	M ⁺ (5.4)	[M + H - H ₂ O] ⁺ (PGA-H) ⁺ (11.1)	-	-	[M - H] ⁻ (100)	M ⁻ (6.2)	[M - H - H ₂ O] ⁻ (PGA-H) ⁻ (100)	-	-	-	-	-	-	

^a Relative abundance of the negative ion whose ac⁻ corresponds to the molecular mass of amino acid M subtracted that of [M - H]⁻ having one isotopic of ¹³C, ¹⁵N, ¹⁸O or ³⁴S.

Table 1. Continued.

Analyte (M)	Proton affinities of M and [M - H] ⁻ (kJ mol ⁻¹)	Ionization energy (eV)	Dipole moment ¹⁴ (Debye)	Ionization reactions	Positive ions (relative abundances [%])				Negative ions (relative abundances [%])									
					Protonation	Molecular cation formation	Fragmentation	Oxidation	Deprotonation	Molecular anion formation	Fragmentation	Oxidation	Hydrogen loss	Attachment of negative background ions R ⁻				
														R ⁻	O ₂ ⁻	HCO ₂ ⁻	NO ₂ ⁻	COO(COOH) ⁻
14. L-Methionine (Met; Mr 149)	925.4 ^a -	8.3 ¹¹	1.84	-	[M + H] ⁺ (100)	M ⁺⁺ (8.7)	-	[M + H + O] ⁺ (5.2)	[M - H] ⁻ (100)	-	-	[M - H + O] ⁻ (13.4)	[M - 2H - H] ⁻ (30.4)	[M + O ₂] ⁻ (33.2)	[M + HCO ₂] ⁻ (11.8)	[M + NO ₂] ⁻ (13.9)	[M + COO(COOH)] ⁻ (11.2)	
 Sulfur-containing aliphatic amino acids																		
15. L-Cysteine (Cys; Mr 121)	902.3 ^a 1399.0 ± 9.6 ¹⁰	9.5 ¹¹	1.99	-	[M + H] ⁺ (100)	M ⁺⁺ (1.8)	-	-	[M - H] ⁻ (100)	-	-	-	[M - 2H - H] ⁻ (15.6)	-	-	-	[M + COO(COOH)] ⁻ (19.8)	
 Polar (neutral)																		
16. L-Phenylalanine (Phe; Mr 165)	922.9 ^a 1408.0 ± 13.0 ¹⁰	8.4 ¹¹	1.32	-	[M + H] ⁺ (100)	M ⁺⁺ (1.7)	-	-	[M - H] ⁻ (100)	M ⁺ (6.8) [*]	-	[M - H + O] ⁻ (8.7)	[M - 2H - H] ⁻ (14.0)	[M + O ₂] ⁻ (12.0)	[M + HCO ₂] ⁻ (7.0)	[M + NO ₂] ⁻ (5.3)	[M + COO(COOH)] ⁻ (15.2)	
 Aromatic amino acids																		
17. L-Tyrosine (Tyr; Mr 181)	926.8 ^a 1413.0 ± 13.0 ¹⁰	-	2.63	-	[M + H] ⁺ (100)	M ⁺⁺ (1.6)	[M + H - CO ₂] ⁺ (5.9)	[M + H + O] ⁺ (4.2)	[M - H] ⁻ (100)	-	-	[M - H + O] ⁻ (6.3)	-	[M + O ₂] ⁻ (63.0)	[M + HCO ₂] ⁻ (36.1)	[M + NO ₂] ⁻ (30.0)	[M + COO(COOH)] ⁻ (13.2)	
 Polar (neutral)																		
18. L-Proline (Pro; Mr 115)	920.5 ^a 1423.0 ± 13.0 ¹⁰	8.3 ¹¹	1.64	-	[M + H] ⁺ (100)	M ⁺⁺ (8.2)	-	-	[M - H] ⁻ (100)	-	-	-	-	[M + O ₂] ⁻ (24.2)	[M + HCO ₂] ⁻ (18.2)	[M + NO ₂] ⁻ (6.9)	[M + COO(COOH)] ⁻ (10.1)	
 Heterocyclic amino acids																		
19. L-Tryptophan (Trp; Mr 204)	948.9 ^a 1409.0 ± 13.0 ¹⁰	8.4 ¹¹	4.18	-	[M + H] ⁺ (100)	M ⁺⁺ (2.9)	-	[M + H + O] ⁺ (8.0)	[M - H] ⁻ (100)	-	-	[M - H + O] ⁻ (17.1)	-	[M + O ₂] ⁻ (62.9)	[M + HCO ₂] ⁻ (45.6)	[M + NO ₂] ⁻ (37.8)	[M + COO(COOH)] ⁻ (14.7)	
 Aromatic heterocyclic amino acids																		
20. L-Histidine (His; Mr 155)	988.0 ^a 1385.0 ± 13.0 ¹⁰	-	3.91	-	[M + H] ⁺ (100)	M ⁺⁺ (4.8)	-	-	[M - H] ⁻ (100)	-	-	[M - H + O] ⁻ (2.1)	-	[M + O ₂] ⁻ (2.4)	-	-	[M + COO(COOH)] ⁻ (26.0)	
 Polar (basic)																		

^aRelative abundance of the negative ion whose m/z corresponds to the molecular mass of analyte M subtracted that of [M - H]⁻ having one isotope of ¹³C, ²H, ¹⁷O or ¹⁵N.



Analytes in DART can be oxidized by hydrogen radicals HO^\bullet via oxygen attachment and hydrogen loss. (17 / 20 words)